Onametostat, a PfPRMT5 inhibitor, exhibits antimalarial activity to *Plasmodium falciparum*

Hui Min,[1,2] Amuza Byaruhanga Lucky,[1] Jesper J. Madsen,[3,4] Anongruk Chim-Ong,[1] Xiaolian Li,[1] Liwang Cui,[1,3] Jun Miao[1,3]

AUTHOR AFFILIATIONS See affiliation list on p. 9.

ABSTRACT   Protein arginine methyltransferases (PRMTs) play critical roles in *Plasmodium falciparum*, a protozoan causing the deadliest form of malaria, making them potential targets for novel antimalarial drugs. Here, we screened 11 novel PRMT inhibitors against *P. falciparum* asexual growth and found that onametostat, an inhibitor for type II PRMTs, exhibited strong antimalarial activity with a half-maximal inhibitory concentration (IC_{50}) value of 1.69 ± 0.04 µM. *In vitro* methyltransferase activities of purified PfPRMT5 were inhibited by onametostat, and a shift of IC_{50} to onametostat was found in the *PfPRTM5* disruptant parasite line, indicating that PfPRTM5 is the primary target of onametostat. Consistent with the function of PfPRMT5 in mediating symmetric dimethylation of histone H3R2 (H3R2me2s) and in regulating invasion-related genes, onametostat treatment led to the reduction of H3R2me2s level in *P. falciparum* and caused the defects on the parasite's invasion of red blood cells. This study provides a starting point for identifying specific PRMT inhibitors with the potential to serve as novel antimalarial drugs.

KEYWORDS   *Plasmodium falciparum*, PRMT, antimalarials, arginine methylation

A ccording to the World Health Organization, despite substantial progress in reducing malaria infections and fatalities over recent decades, the disease remains one of the most pressing global health challenges, with an estimated 249 million cases and 608,000 deaths in 2022 (1). Nowadays, artemisinin-based combination therapies (ACTs) are widely adopted as the frontline antimalarial drugs. However, the emergence of drug resistance to ACTs threatens the progress made in malaria control, emphasizing the necessity for novel classes of antimalarials that can be used in combination therapies (2, 3). These innovative drugs may be discovered by screening compound libraries against cultured parasites or isolated target molecules validated as essential for parasite viability (4–6). Importantly, to delay or prevent the development of drug resistance, the potential compound should ideally target novel biological activities in the parasite. Recently, extensive high-throughput phenotypic screening has been conducted for the development of antimalarial drugs (7–10).

Epigenetic regulation is a crucial mechanism that contributes to the regulation of gene expression. This process involves remodeling the chromatin structure between active and silent states through various mechanisms, including reversible histone modifications (11). Arginine methylation is a post-translational modification that affects many cellular processes in eukaryotes and plays an important role in many cellular processes, such as RNA processing, signal transduction, and transcription (12, 13). Arginine methylation is catalyzed by a family of protein arginine methyltransferases (PRMTs), which can add one or two methyl groups from S-adenosylmethionine (SAM) to the guanidine–nitrogen of arginine, resulting in three major forms of methylated arginines: MMA–ω-N^G-monomethylarginine, aDMA–asymmetric ω-N^G,N^G-dimethylarginine, or sDMA–symmetric ω-N^G, N^G-dimethylarginine) (13). Types I and II PRMTs catalyze

the formation of aDMA and sDMA, respectively. PRMT1 and PRMT5, as the main type I and II enzymes, generate repressive histone markers (H3R8me2s and H4R3me2s) as well as active markers (H4R3me2a and H3R2me2s), respectively (13–15). In addition, PRMTs also deposit arginine methylation on non-histone substrates, regulating essential cellular processes such as transcription, cell signaling, mRNA translation, and pre-mRNA splicing (16). PRMTs play key roles in RNA splicing, cell differentiation, and development and link to diseases such as cancer (17–19). Recently, arginine methylation has attracted increasing attention as a key post-translational modification (PTM), which can be utilized as a therapy for neurodegenerative diseases and cancer (13, 20–22).

Plasmodium spp. rely heavily on epigenetic mechanisms to drive both asexual proliferation and sexual differentiation (23–25). *Plasmodium* histones carry a myriad of PTMs, such as methylation, acetylation, phosphorylation, ubiquitylation, and SUMOy-lation (26–32). The malaria parasite *Plasmodium falciparum* encodes three conserved PRMTs, namely, PRMT1, PRMT4 (also known as CARM1), and PRMT5 (33–35). Our previous studies showed that PfPRMT1 is a type I PRMT located in the nucleus and cytoplasm with activities toward histones and non-histone substrates (34). Recently, PfPRMT5, a type II PRMT, was found to play a critical role in RNA splicing and regulating the invasion of red blood cells (RBCs), partially due to its activation of invasion genes by creating H3R2me2s
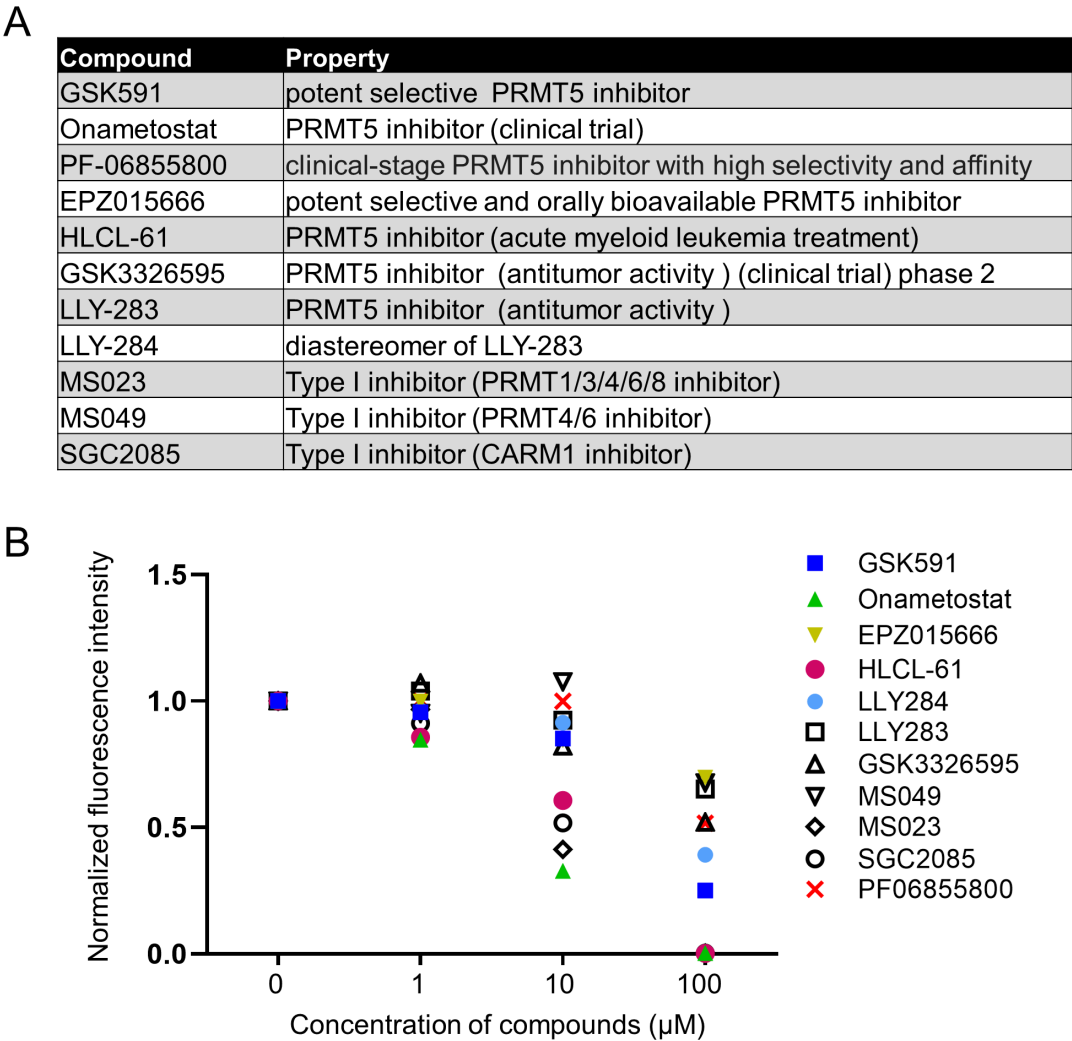

FIG 1 Screening 11 PRMT5 inhibitors in *P. falciparum*. (A) Eleven commercially available PRMT inhibitors were selected. Among them, eight compounds are potent PRMT5 inhibitor candidates. (B) All the compounds were screened for *in vitro* activity against asexual *P. falciparum* parasites at 0, 1, 10, and 100 µM, respectively.

in the corresponding promoters (36). Therefore, PfPRMTs are promising targets for antimalarials.

Epigenetic inhibitors hold promise as antimalarials, with several studies involving a limited number of such inhibitors demonstrating activity against one or more stages of malaria parasites (37–39). However, the impact of PRMT inhibitors on malaria parasites has not been evaluated yet. In the present study, we screened 11 commercially available PRMT inhibitors to determine their potential antimalarial activity. We found that onametostat, a type II PRMT inhibitor, had the strongest antimalarial activity among the tested compounds. Furthermore, onametostat inhibited PfPRMT5 methyltransferase activities and blocked parasite growth by reducing the level of H3R2me2s and impairing the parasite's invasion capacity. Additionally, the inhibitory activity of onametostat was attenuated upon *PfPRMT5* gene disruption.

RESULTS

Screening PRMT inhibitors in *P. falciparum*

Based on the studies of PRMT inhibitors against enzymatic activities in the cell-free system, cancer cell lines, or animal models, we selected three type I PRMT inhibitors (MS023 [40], MS049 [41], and SGC2085 [42]) and eight type II PRMT inhibitors (GSK591 [43], GSK-3326595 [44], onametostat [45], PF-06855800 [46], EPZ015666 [47], HLCL-61 [48], LLY-283, and LLY-284 [49]), which showed highly potent inhibitory activities (Fig. 1A). Among them, GSK-3326595, onametostat, and PF-06855800 are being assessed in clinical trials (46, 50).

To assess the activity of the PRMT inhibitors against *P. falciparum*, we performed *in vitro* growth inhibition assays against asexual-stage parasites at 0, 1, 10, and 100 µM of each compound. At 10 µM, MS023 and onametostat inhibited parasite growth by over 50%, whereas SGC2085 and HLCL-61 showed near 50% growth inhibitory activities (Fig. 1B). At 100 µM, these four compounds almost completely inhibited parasite growth, with the fluorescence intensity approaching zero (Fig. 1B).

To further validate the activities of MS023, SGC2085, onametostat, and HLCL-61, we determined their IC_{50} values against parasite strain 3D7 using the *in vitro* SYBR green-based drug assay (Fig. 2). HLCL-61 and SGC2085 showed weak inhibitory activities with IC_{50}s at 21.14 ± 3.21 and 15.69 ± 1.75 µM, respectively. MS023 demonstrated a modest antimalarial activity with an IC_{50} value of 9.86 ± 0.95 µM. Onametostat exhibited the strongest activity, with an IC_{50} value of 1.69 ± 0.04 µM. Thus, from the 11 PRMT inhibitors, onametostat was identified as the most potent compound against asexual growth of the malaria parasite.

Modeling onametostat binding to PfPRMT5

The IC_{50}s of onametostat in six lung cancer cell lines were at a low nanomolar range (0.4–1.9 nM), significantly lower than the IC_{50} of onametostat in *P. falciparum* (45). Sequence alignment shows that the PfPRMT5 catalytic domain displays high sequence identity/similarity to HsPRMT5 (44/64%) (36). Recently, the co-crystal structure of onametostat bound to the active site of HsPRMT5 (PDB ID: 6RLQ) has been solved, showing that onametostat closely binds several amino acids in the active site (45) (Fig. 3A). Interestingly, almost all respective amino acids are conserved in PfPRMT5 except for M420 in HsPRMT5, which is I507 in PfPRMT5 (Fig. S1).

To fully appreciate this conservation and variation, we explored the differences in onametostat interaction with HsPRMT5 and PfPRMT5 by modeling the known structure of onametostat interaction with HsPRMT5. In the crystal structure of onametostat bound to HsPRMT5, the bromo-aminoquinoline moiety occupies the substrate-binding site, establishing bidentate hydrogen-bonding interactions with the catalytic E444 (E531 in PfPRMT5) (Fig. 3A). Additionally, the bromine atom of onametostat engages in a halogen interaction with the backbone oxygen atom of S578 (S665 in PfPRMT5), and F327 (F390 in PfPRMT5) forms a π–π stacking interaction with onametostat, capping this region of
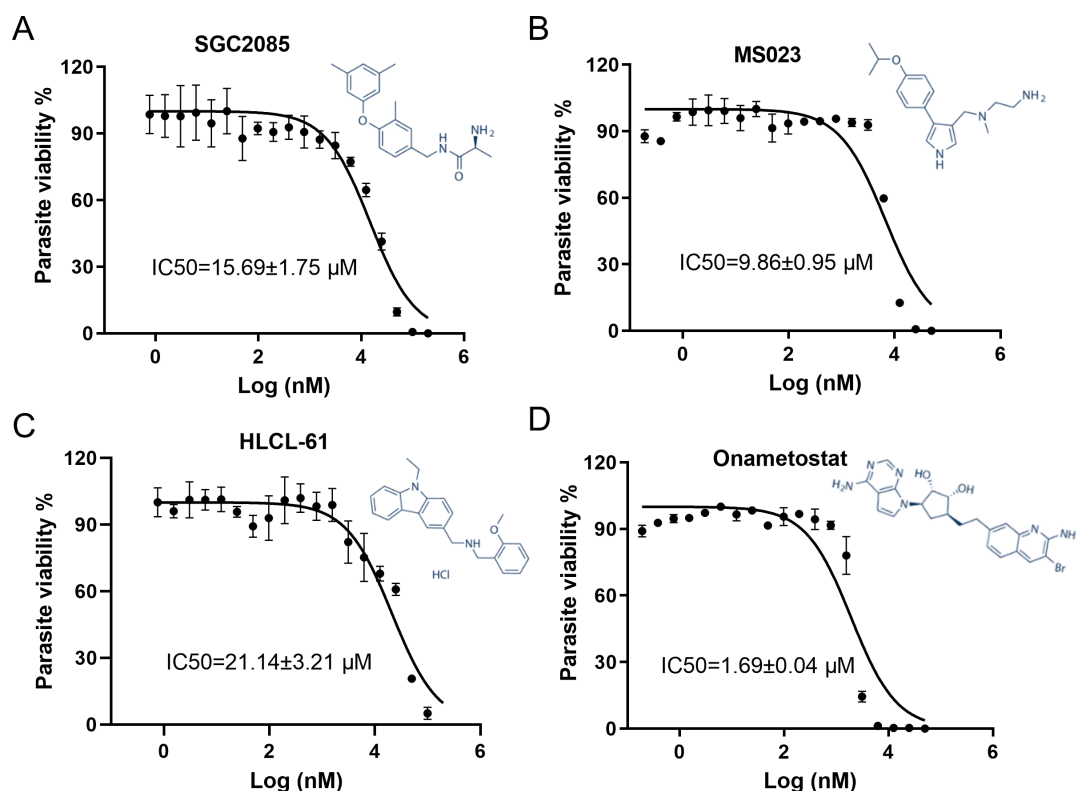
FIG 2 Inhibition curves of PRMT inhibitors against *P. falciparum*. The asexual growth inhibition assay results for SGC2085 (A), MS023 (B), HLCL-61 (C), and onametostat (D) are presented as IC_{50} values. The chemical structures of compounds are shown on the right panel.

the inhibitor (Fig. 3A). The central dihydroxycyclopentane moiety of onametostat forms bidentate hydrogen bonds with E392 (E479 in PfPRMT5) and a hydrogen bond with Y324 (Y387 in PfPRMT5), while also coordinating with a water molecule (Fig. 3A). Although the distance to K393 (K480 in PfPRMT5) is relatively large at 4.0 Å, limiting its interaction with the central group, this residue engages in a cation–π interaction with the pyrrolopyrimidine moiety of onametostat. Notably, the interaction with the enzyme around the pyrrolopyrimidine group involves a hydrogen bond to the backbone nitrogen atom of M420 (I507 in PfPRMT5) (Fig. 3A). However, differences arise in the interaction between onametostat and HsPRMT5 versus PfPRMT5, particularly concerning the hydrophobic environment surrounding the pyrrolopyrimidine group. This interaction involves M420/I507, which contributes to the hydrophobic milieu where the pyrrolopyrimidine moiety nests. Structural analysis reveals differences in this hydrophobic neighborhood around M420/I507, including substitutions of V391 by I478, L364 by V450, and A453 by I540 (Fig. 3B). These differences likely contribute to distinct affinity profiles, offering a potential avenue for further exploration and optimization.

Specific targeting of PfPRMT5 by onametostat

To experimentally confirm that onametostat can specifically inhibit PfPRMT5, we investigated the inhibitory effects of onametostat on PfPRMT5 methyltransferase activities. We first purified PfPRMT5 from the PfPRMT5::PTP parasite line by tandem affinity purification (TAP) procedure as shown in our previous pulldown (36, 51) (Fig. S2A). The purified PfPRMT5 was functional and showed high activities by *in vitro* methyltransferase assay (Fig. S2B). Adding onametostat into the reaction mixture at 1:1 and 1:2 molar ratio of PfPRMT5 to onametostat resulted in ~48% and ~66% reduction of its activities, respectively (Fig. 4A; Fig. S2C), indicating that onametostat could directly inhibit PfPTMT5 activity. Disruption of target genes will dampen the inhibitory effects
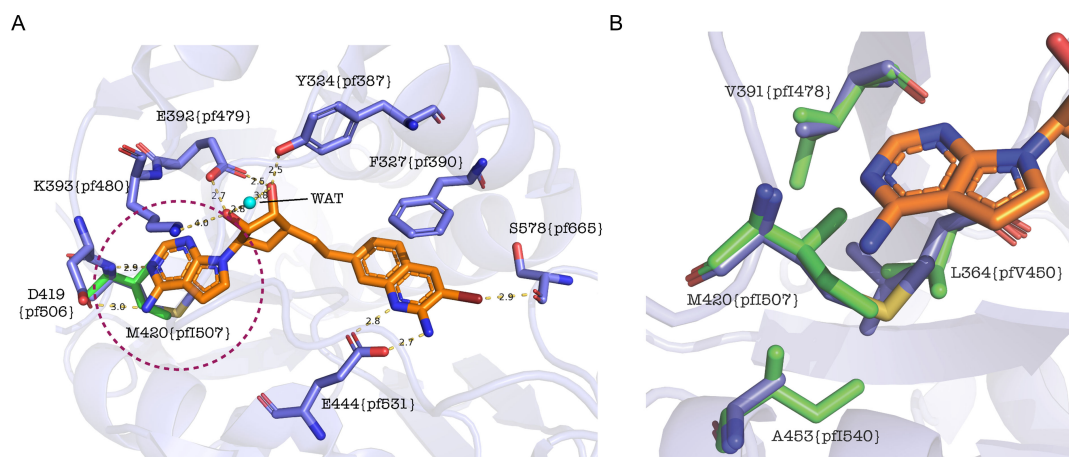
FIG 3 *In silico* modeling shows the binding of onametostat to PfPRMT5. Structural interactions between HsPRMT5 and PfPRMT5 with onametostat are shown. Onametostat is in the stick form (orange). The protein backbone is represented with a ribbon diagram, and crucial amino acids directly interacting with onametostat are illustrated as sticks (blue for Hs; green for Pf). Distances of significance are denoted by dashed lines (yellow), while a coordinating water molecule is visualized as a sphere (cyan). Residue nomenclature adheres to Hs, with the corresponding position in Pf denoted in curly brackets. (A) General interaction mode between onametostat and HsPRMT5, with the sole distinction in PfPRMT5's interaction highlighted within the dashed circle region. This discrepancy involves the substitution of M420 to I507. (B) A magnified perspective of the distinct region and the adjacent hydrophobic environment.

of the respective drugs (6, 52). Therefore, we anticipated that disruption of *Pf*PRMT5 would lessen onametostat's inhibitory activity. As expected, the IC_{50} of onametostat in the *PfPRMT5* disruptant line was increased >2-fold (3.88 ± 1.61 µM) compared to the wild-type parasite, whereas the IC_{50} of onametostat in an unrelated gene disruption line, *PfDNMT2* disruption line (53), did not change compared to its wild-type control (Fig. 4B; Fig. S2D).

Our recent studies showed that PfPRMT5 regulated gene expression by depositing the active histone marker, H3R2me2s, in the promoters of target genes, including certain invasion genes at the schizont stage, and disruption of *PfPRMT5* resulted in the reduction of H3R2me2s and defects in the invasion of RBCs (36). To investigate whether onametostat targets PfPRMT5, onametostat at the IC_{50} concentration was added to highly synchronized schizont-stage parasites for 3 h. Compared to the DMSO control, the level of H3R2me2s was significantly reduced following onametostat treatment (Fig. 4C). When highly synchronized ring-stage parasites were incubated with onametostat at the IC_{50} concentration, no dead parasites were detected during the intraerythrocytic developmental cycle (Fig. S3). The egress process of schizonts was normal under onametostat treatment at either IC_{50} or IC_{90} (Fig. 4D), suggesting that onametostat did not block the parasite development and might instead impair the merozoite invasion process. Therefore, we quantified the invasion rates and found that onametostat treatment at IC_{50} or IC_{90} significantly reduced the parasite's invasion rate (Fig. 4E). Collectively, these results showed that onametostat impaired the parasite asexual stage growth by specifically targeting PfPRMT5.

DISCUSSION

This study investigated 11 inhibitors known to target mammalian PRMTs for their antimalarial activities against the asexual stages of *P. falciparum*. We showed that the selective PRMT5 inhibitor, onametostat, exhibited significant anti-proliferative efficacy against asexual *P. falciparum* parasites and specifically inhibited type II PRMT (PfPRMT5) activities.

Many compounds potentially targeting epigenetic modulators have been proven active against cancerous cells (54, 55). Notably, PRMT5 inhibitors have shown promising results in clinical trials for treating certain types of tumors (56–58). A growing body of literature has demonstrated that epigenetic regulation is becoming an attractive
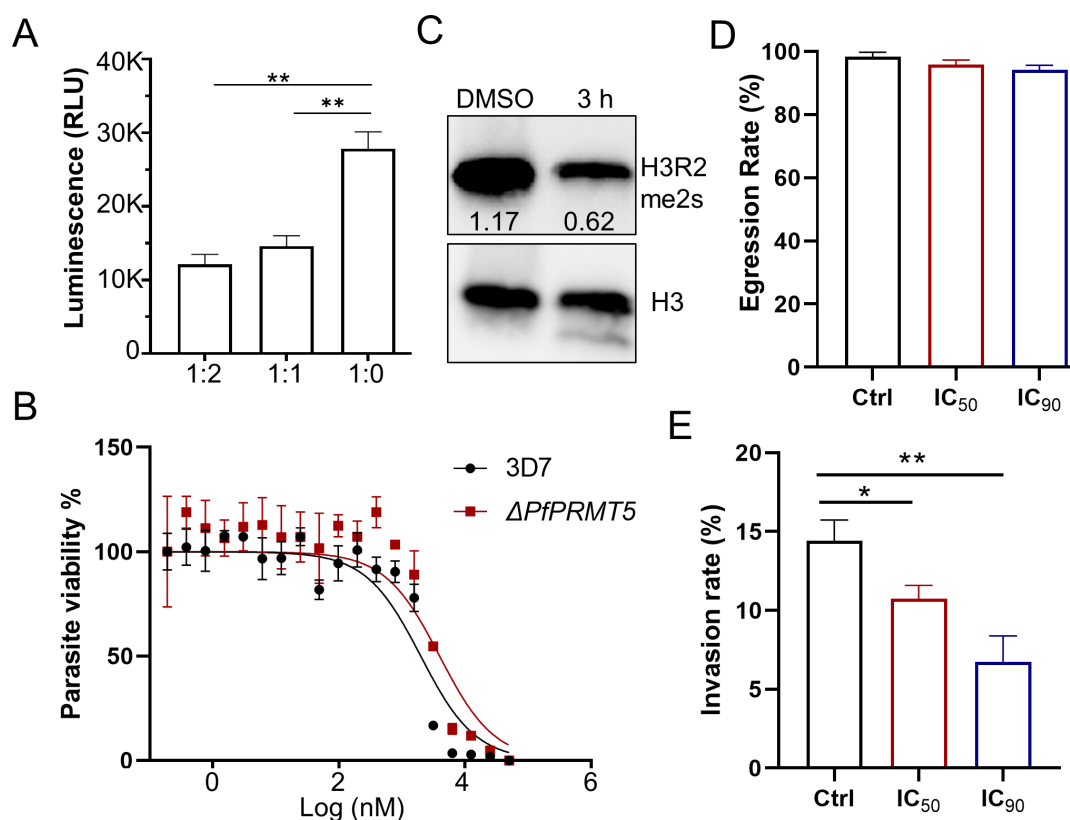
FIG 4 The effects of onametostat on *P. falciparum*. (A) The activity of the purified PfPRMT5 was significantly inhibited by onametostat at a molar ratio of 1:1 and 1:2 of PRMT5 to onametostat. The activities were measured using *in vitro* methyltransferase activity assays and shown as relative light units (RLU). (B) Comparison of the *in vitro* susceptibility of *ΔPfPRMT5* parasite line with 3D7 exposed to onametostat. (C) The level of H3R2me2s was detected by Western blot after parasites at the schizont stage were treated with either dimethyl sulfoxide (DMSO) or onametostat at IC$_{50}$ for 3 h. H3 was used as a loading control. The numbers show the relative levels of H3R2me2s normalized with H3. (D) Onametostat at IC$_{50}$ and IC$_{90}$ did not significantly disturb schizont egress. The egress rate was defined as the ratio of naturally ruptured mature schizonts from three replicates. (E) Onametostat at IC$_{50}$ and IC$_{90}$ concentrations substantially disturbed merozoite invasion. Invasion rates of parasites were estimated using purified schizonts. Error bars in all panels indicate the mean ± SD from three replicates. *$P < 0.05$, **$P < 0.01$.

molecular target in the design of novel antimalarials (38, 59). Recently, epigenetics drugs were screened for activities against the asexual or sexual stages of cultured *P. falciparum*, including histone deacetylases, histone lysine methyltransferases, and PRMT inhibitors, but no lead compounds were identified (37, 39). In this study, four of the 11 selected PRMT inhibitors inhibited parasite proliferation by ~50% at 10 µM, with onametostat displaying the most potent activity at an IC$_{50}$ value of 1.69 µM.

Onametostat inhibits PRMT5 activity by binding non-covalently in the SAM binding site and substrate-binding pockets(45). It is a highly selective PRMT5 inhibitor, with a high binding affinity to PRMT5 and a Kd of ≤1 nmol/L in human lung cancer cell lines. The catalytic domain of PfPRMT5 exhibits 44% sequence identity and 64% sequence similarity to HsPRMT5/JBP1 (36). Notably, among the amino acids in HsPRMT5 directly interacting with onametostat, only one is not conserved in PfPRMT5 (Fig. S1). Detailed structural analysis suggested that onametostat specifically targeted the catalytic domain of PfPRMT5 but with relatively lower inhibition activity against *Plasmodium* parasites compared to cancer cells.

Our recent study showed that PfPRMT5 catalyzes the formation of symmetrical methylation of H3R2 to mediate transcriptional activation in *P. falciparum* (36). H3R2me2s was enriched in the promoters of certain genes, including invasion genes, and disruption of *PfPRMT5* resulted in defects in merozoite invasion of RBCs. Furthermore, PfPRMT5 is also associated with invasion-related transcriptional regulators, such as AP2-I and

RNA splicing machinery, which play key roles in regulating splicing of many RNA species including those encoding invasion-related genes (36). In this study, onametostat could inhibit PfPRMT5 activity by *in vitro* methyltransferase assay. Additionally, onametostat specifically reduced the level of H3R2m2s and invasion capacity in the wild-type parasite, and the PfPRMT5 disruptant line became less sensitive to onametostat. All these demonstrate that onametostat is a specific inhibitor of PfPRMT5. It is anticipated that onametostat also disturbs RNA splicing by inhibition of PfPRMT5 in *P. falciparum*.

Besides onametostat, the other three PRMT5 inhibitors tested in this study, namely MS023, SGC2085, and HLCL-61, inhibited parasite growth at a low micrometer range (~10–20 µM), underscoring the significance of PfPRMTs as the promising drug targets. Further detailed analyses of drug–PRMT interactions and inhibition phenotypes are needed to facilitate rational drug design and optimization.

MATERIALS AND METHODS

Parasite culture

The *P. falciparum* parasites were cultured in type O^+ human RBCs at 5% hematocrit in RPMI 1640 medium supplemented with 25 mM HEPES, 50 mg/L of hypoxanthine, 25 mM $NaHCO_3$, 0.5% Albumax II, and 40 mg/mL of gentamicin sulfate. The deidentified and anonymous human blood was purchased from BioIVT. The culture was maintained at 37°C in a gas mixture of 5% CO_2, 3% O_2, and 92% N_2. The *ΔPfPRMT5* parasite line was generated earlier (36). For synchronization, the culture was initiated with purified parasites using a Percoll step gradient, and the ring-stage parasites were treated with 5% sorbitol.

In vitro drug sensitivity assay

The *in vitro* susceptibilities of the wild-type and mutant parasites to 11 PRMT inhibitors were tested using the SYBR green I-based assay (60). Briefly, synchronized ring-stage parasites were cultured with each selected compound at 1% hematocrit and 0.5% parasitemia in a 96-well plate. Each compound at each concentration was applied in two wells (two technical replicates). Wells with no drug and only RBCs were used as a positive control and the background, respectively. After 72 h of incubation, the cells in the plates were frozen, thawed, and then lysed using 100 µL of lysis buffer (20 mM Tris-HCl, [pH 7.5], 5 mM EDTA, 0.08% Triton X-100, 0.008% saponin in phosphate buffered saline [PBS], and 0.2 µL of SYBR green I). The plates were incubated at 37°C for 1 h in the dark after thorough mixing, and fluorescence intensities in each well were measured using a spark multimode microplate reader (TECAN). For each drug, the array was performed three times independently at three separate time points. The values from these three replicates were used for calculating the percentage of parasite growth against the control after subtracting the RBC background signal. IC_{50} and IC_{90} values were calculated using Prism 8 (GraphPad Software Inc.) by fitting a curve with nonlinear regression (sigmoidal dose–response/variable slope equation).

The PRMT5 inhibitor PF-06855800 was purchased from ChemieTek, while the rest of the PRMT inhibitors were from Selleck Chemicals. The stock solutions were prepared with DMSO to a concentration of 5 or 10 mg/mL. To screen the inhibitors' effects on *P. falciparum*, each compound was tested at a concentration of 1, 10, or, 100 µM. Parasites treated with the solvent DMSO were used as controls. To determine the IC_{50} of onametostat, HLCL-61, MS023, and SGC2085 synchronized ring-stage 3D7 or *ΔPfPRMT5* parasites were cultured with serial dilutions of each drug in a 19-point dose–response gradient (concentration range, 0.019 nM to 50 µM).

Structural modeling

The structural configuration of HsPRMT5 and its inhibition by onametostat have been elucidated through the co-crystal structure with PDB ID: 6RLQ (45). For comparative

analysis, the PfPRMT5 structure was modeled by employing 6RLQ as a template using SWISS-MODEL web server (61). The default parameters and settings of the SWISS-MODEL were used. Additionally, structure prediction for PfPRMT5 was performed using AlphaFold2 (62, 63), to validate the template-based model. With the substantial sequence identity of PfPRMT5 to the template, both the template-based and AlphaFold2-predicted models exhibited minimal structural deviation compared with the HsPRMT5 template (root-mean-square deviation for the methyltransferase domain was 0.146 and 0.424 Å over 132 and 130 alpha-carbon atoms, respectively). The structural models were examined using PyMOL (Version 2.5.0, Schrödinger LLC) for visual inspection and verification.

Purification of histones and PfPRMT5

Histones were isolated from the schizont stage of synchronized parasites as described previously (36). Parasites were harvested with saponin lysis. The parasite pellets were washed with cold PBS till the supernatant was clear. Then, the pellet was resuspended in a hemoglobin-removal buffer (25 mM Tris–HCl, pH 7.8, 1 mM EDTA, 0.2% Nonidet P40) to remove hemoglobin. After washing with 0.8 M NaCl two times, the histones were extracted with 0.25 M HCl and incubated at 4℃ for 3 h. Acid-soluble fractions were pooled and mixed with equal volumes of 20% tri-chloroacetic acid and incubated on ice for 30 min. Histones were precipitated by centrifugation at $12,000 \times g$ for 15 min at 4℃, washed with 500 µL of acetone, dried, and dissolved in an SDS-PAGE sample buffer.

PfPRMT5 was purified from the PfPRMT5::PTP parasite line by the established TAP procedure (36, 51). Briefly, ~5×10^8 synchronized schizonts were lysed in the PA150 buffer. The lysate was centrifuged for 10 min at $16,000 \times g$, and the supernatant was incubated with IgG agarose beads (100 µL, GE Healthcare) at 4℃ for 2 h. The beads were equilibrated with the TEV buffer. and PfPRMT5-PTP was released from beads by digestion with TEV protease (150 U) overnight at 4 ℃. The supernatant was collected and incubated with anti-protein C beads for 2 h at 4℃. The proteins that bound to the beads were eluted with an elution buffer. The final eluate was collected for *in vitro* methyltransferase assay.

Western blots

An equal volume of the wild-type 3D7 parasites at the schizont stage was treated with either DMSO or onametostat for 3 h. After treatment, parasites were harvested, and their histones were extracted as described above. Protein concentration was measured using the Pierce BCA Protein Assay Kit (Thermo Fisher Scientific). The purified histones were separated by 10% SDS-PAGE and transferred to nitrocellulose membranes. Western blotting was performed using a standard procedure with rabbit anti-histone H3R2 dimethyl symmetric (H3R2me2s) (1:1,000, Epigentek), which was verified by dot blots in our recent PfPRMT5 functional study (36), as the primary antibodies and horseradish peroxidase-conjugated goat anti-rabbit IgG (1:3,000) as the secondary antibodies. Rabbit anti-H3 (1:1,000, Epigentek) was used as the loading control. The results were visualized using the ECL detection system to confirm the PfPRMT5 was pulled down by TAP from PfPRMT5::PTP parasites. The elute from TAP was separated by 10% SDS-PAGE followed by Western blots with anti-protein C antibodies (1:1,000, GenScript).

In vitro methyltransferase assay

Methyltransferase activity of PfPRMT5 and inhibitor assay were performed using the MTase-Glo assay (Cat. No. V7601, Promega) following the manufacturer's protocol (64). For the enzyme activity assay, serial dilutions of PfPRMT5 ranging from 50 to 0.05 µg or no protein as control were incubated in the presence of 0.1 µM human recombinant mononucleosomes (rNucs) (Cat. No. 16–0009, EpiCypher) in reaction buffer (80 mM Tris pH 8.0, 200 mM NaCl, 4 mM EDTA, 12 mM $MgCl_2$, 0.4 mg/mL of BSA, 4 mM dithiothreitol), along with 10 µM S-adenosylmethionine (SAM). The total reaction volume

was 20 µL, and incubation was performed for 60 min at 37°C in 96-well plates (Cat. No. 15042, Pierce). After incubation, 5 µl of 5 × MTase Glo Reagent (Promega) was added followed by shaking for 2 min at 1,000 rpm and additional incubation at room temperature for 30 min. Subsequently, 25 µl of MTase-Glo Detection Solution (Promega) was added, and the plates were shaken again for 2 min and incubated for another 30 min at room temperature. Luminescence was measured as relative light units (RLU) using a spark multimode microplate reader (TECAN). For inhibitor activity assay, purified PfPRMT5 was pre-incubated with varying concentrations of onametostat or DMSO as a control for 30 min before adding the remaining components. The assay wells received 17.5 µL of reaction buffer containing 115 µM PfPRMT5 and onametostat at molar ratios of 1:2, 1:1, and 1:0, followed by 30 min of incubation at 37°C. Then, 12.5 L of reaction buffer, containing SAM (10 µM) and rNucs (0.1 µM), along with 5 µL of 5 × MTase Glo Reagent, were added. The reactions were incubated for 60 min at 37°C, and then 30 µL of MTase-Glo Detection Solution was added, followed by a 30-min incubation at room temperature. Luminescence was quantified shortly after addition. Data were expressed as relative luminescence by subtracting the luminescence from a negative control reaction without onametostat.

In vitro evaluation of parasite egress and invasion

To assess the impact of onametostat treatment on parasite egress, highly synchronized mature schizonts were exposed to onametostat at IC_{50} and IC_{90} concentrations. Egress rate was defined as the proportion of mature schizonts that naturally ruptured. The invasion assay was performed as previously described (36). Purified mature schizonts were incubated with RBCs to allow schizont rupture and re-invasion. Ring-infected erythrocytes were counted after Giemsa staining. All the assays are performed in triplicate.

Statistical analysis

Phenotypic comparisons between 3D7 and *ΔPfPRMT5* parasite lines were carried out using GraphPad Prism, version 8.0. The egress and invasion rates in the onametostat treatment groups were compared with the control using one-way analysis of variance (ANOVA). Dunnett's multiple comparison test was employed for multiple comparisons. Data are represented as mean ± standard deviation (SD) from three independent experiments. Unless indicated otherwise, $P < 0.05$ was taken as statistically significant.

AUTHOR AFFILIATIONS

[1]Department of Internal Medicine, Morsani College of Medicine, University of South Florida, Tampa, Florida, USA

[2]Department of Immunology, College of Basic Medical Sciences, China Medical University, Shenyang, China

[3]Center for Global Health and Infectious Diseases Research, College of Public Health, University of South Florida, Tampa, Florida, USA

[4]Department of Molecular Medicine, Morsani College of Medicine, University of South Florida, Tampa, Florida, USA

AUTHOR ORCIDs

Liwang Cui http://orcid.org/0000-0002-8338-1974

Jun Miao http://orcid.org/0000-0001-9374-6749

FUNDING

AUTHOR CONTRIBUTIONS

ADDITIONAL FILES

The following material is available online.

Supplemental Material

Supplemental figures (AAC00176-24-s0001.pdf). Figures S1 to S3.

REFERENCES

1. WHO. 2023. Would malaria report 2023. WHO, Geneva.
2. Haldar K, Bhattacharjee S, Safeukui I. 2018. Drug resistance in *Plasmodium*. Nat Rev Microbiol 16:156–170. https://doi.org/10.1038/nrmicro.2017.161
3. Balikagala B, Fukuda N, Ikeda M, Katuro OT, Tachibana S-I, Yamauchi M, Opio W, Emoto S, Anywar DA, Kimura E, Palacpac NMQ, Odongo-Aginya EI, Ogwang M, Horii T, Mita T. 2021. Evidence of artemisinin-resistant malaria in Africa. N Engl J Med 385:1163–1171. https://doi.org/10.1056/NEJMoa2101746
4. Cabrera AC. 2019. Collaborative drug discovery and the Tres Cantos Antimalarial Set (TCAMS). Drug Discov Today 24:1304–1310. https://doi.org/10.1016/j.drudis.2019.04.005
5. Forte B, Ottilie S, Plater A, Campo B, Dechering KJ, Gamo FJ, Goldberg DE, Istvan ES, Lee M, Lukens AK, McNamara CW, Niles JC, Okombo J, Pasaje CFA, Siegel MG, Wirth D, Wyllie S, Fidock DA, Baragaña B, Winzeler EA, Gilbert IH. 2021. Prioritization of molecular targets for antimalarial drug discovery. ACS Infect Dis 7:2764–2776. https://doi.org/10.1021/acsinfecdis.1c00322
6. Siqueira-Neto JL, Wicht KJ, Chibale K, Burrows JN, Fidock DA, Winzeler EA. 2023. Antimalarial drug discovery: progress and approaches. Nat Rev Drug Discov 22:807–826. https://doi.org/10.1038/s41573-023-00772-9
7. Yahiya S, Rueda-Zubiaurre A, Delves MJ, Fuchter MJ, Baum J. 2019. The antimalarial screening landscape-looking beyond the asexual blood stage. Curr Opin Chem Biol 50:1–9. https://doi.org/10.1016/j.cbpa.2019.01.029
8. Dorjsuren D, Eastman RT, Wicht KJ, Jansen D, Talley DC, Sigmon BA, Zakharov AV, Roncal N, Girvin AT, Antonova-Koch Y, et al. 2021. Chemoprotective antimalarials identified through quantitative high-throughput screening of *Plasmodium* blood and liver stage parasites. Sci Rep 11:2121. https://doi.org/10.1038/s41598-021-81486-z
9. Challis MP, Devine SM, Creek DJ. 2022. Current and emerging target identification methods for novel antimalarials. Int J Parasitol Drugs Drug Resist 20:135–144. https://doi.org/10.1016/j.ijpddr.2022.11.001
10. Plouffe DM, Wree M, Du AY, Meister S, Li F, Patra K, Lubar A, Okitsu SL, Flannery EL, Kato N, Tanaseichuk O, Comer E, Zhou B, Kuhen K, Zhou Y, Leroy D, Schreiber SL, Scherer CA, Vinetz J, Winzeler EA. 2016. High-throughput assay and discovery of small molecules that interrupt malaria transmission. Cell Host Microbe 19:114–126. https://doi.org/10.1016/j.chom.2015.12.001
11. Zhang L, Lu Q, Chang C. 2020. Epigenetics in health and disease. Adv Exp Med Biol 1253:3–55. https://doi.org/10.1007/978-981-15-3449-2_1
12. Guccione E, Richard S. 2019. The regulation, functions and clinical relevance of arginine methylation. Nat Rev Mol Cell Biol 20:642–657. https://doi.org/10.1038/s41580-019-0155-x
13. Blanc RS, Richard S. 2017. Arginine methylation: the coming of age. Mol Cell 65:8–24. https://doi.org/10.1016/j.molcel.2016.11.003
14. Migliori V, Müller J, Phalke S, Low D, Bezzi M, Mok WC, Sahu SK, Gunaratne J, Capasso P, Bassi C, Cecatiello V, De Marco A, Blackstock W, Kuznetsov V, Amati B, Mapelli M, Guccione E. 2012. Symmetric dimethylation of H3R2 is a newly identified histone mark that supports euchromatin maintenance. Nat Struct Mol Biol 19:136–144. https://doi.org/10.1038/nsmb.2209
15. Yuan C-C, Matthews AGW, Jin Y, Chen CF, Chapman BA, Ohsumi TK, Glass KC, Kutateladze TG, Borowsky ML, Struhl K, Oettinger MA. 2012. Histone H3R2 symmetric dimethylation and histone H3K4 trimethylation

are tightly correlated in eukaryotic genomes. Cell Rep 1:83–90. https://doi.org/10.1016/j.celrep.2011.12.008

16. Al-Hamashi AA, Diaz K, Huang R. 2020. Non-histone arginine methylation by protein arginine methyltransferases. Curr Protein Pept Sci 21:699–712. https://doi.org/10.2174/1389203721666200507091952

17. Li Z, Yu J, Hosohama L, Nee K, Gkountela S, Chaudhari S, Cass AA, Xiao X, Clark AT. 2015. The Sm protein methyltransferasePRMT5 is not required for primordial germ cell specification in mice. EMBO J 34:748–758. https://doi.org/10.15252/embj.201489319

18. Liu F, Cheng G, Hamard P-J, Greenblatt S, Wang L, Man N, Perna F, Xu H, Tadi M, Luciani L, Nimer SD. 2015. Arginine methyltransferase PRMT5 is essential for sustaining normal adult hematopoiesis. J Clin Invest 125:3532–3544. https://doi.org/10.1172/JCI81749

19. Bezzi M, Teo SX, Muller J, Mok WC, Sahu SK, Vardy LA, Bonday ZQ, Guccione E. 2013. Regulation of constitutive and alternative splicing by PRMT5 reveals a role for Mdm4 pre-mRNA in sensing defects in the spliceosomal machinery. Genes Dev 27:1903–1916. https://doi.org/10.1101/gad.219899.113

20. Wang S-CM, Dowhan DH, Muscat GEO. 2019. Epigenetic arginine methylation in breast cancer: emerging therapeutic strategies. J Mol Endocrinol 62:R223–R237. https://doi.org/10.1530/JME-18-0224

21. Kaneb HM, Dion PA, Rouleau GA. 2012. The FUS about arginine methylation in ALS and FTLD. EMBO J 31:4249–4251. https://doi.org/10.1038/emboj.2012.291

22. Wu Q, Schapira M, Arrowsmith CH, Barsyte-Lovejoy D. 2021. Protein arginine methylation: from enigmatic functions to therapeutic targeting. Nat Rev Drug Discov 20:509–530. https://doi.org/10.1038/s41573-021-00159-8

23. Hollin T, Gupta M, Lenz T, Le Roch KG. 2021. Dynamic chromatin structure and epigenetics control the fate of malaria parasites. Trends Genet 37:73–85. https://doi.org/10.1016/j.tig.2020.09.003

24. Duraisingh MT, Skillman KM. 2018. Epigenetic variation and regulation in malaria parasites. Annu Rev Microbiol 72:355–375. https://doi.org/10.1146/annurev-micro-090817-062722

25. Hollin T, Chahine Z, Le Roch KG. 2023. Epigenetic regulation and chromatin remodeling in malaria parasites. Annu Rev Microbiol 77:255–276. https://doi.org/10.1146/annurev-micro-032521-041554

26. Miao J, Fan Q, Cui L, Li J, Li J, Cui L. 2006. The malaria parasite *Plasmodium falciparum* histones: organization, expression, and acetylation. Gene 369:53–65. https://doi.org/10.1016/j.gene.2005.10.022

27. Trelle MB, Salcedo-Amaya AM, Cohen AM, Stunnenberg HG, Jensen ON. 2009. Global histone analysis by mass spectrometry reveals a high content of acetylated lysine residues in the malaria parasite *Plasmodium falciparum*. J Proteome Res 8:3439–3450. https://doi.org/10.1021/pr9000898

28. Saraf A, Cervantes S, Bunnik EM, Ponts N, Sardiu ME, Chung D-W, Prudhomme J, Varberg JM, Wen Z, Washburn MP, Florens L, Le Roch KG. 2016. Dynamic and combinatorial landscape of histone modifications during the intraerythrocytic developmental cycle of the malaria parasite. J Proteome Res 15:2787–2801. https://doi.org/10.1021/acs.jproteome.6b00366

29. Coetzee N, Sidoli S, van Biljon R, Painter H, Llinás M, Garcia BA, Birkholtz L-M. 2017. Quantitative chromatin proteomics reveals a dynamic histone post-translational modification landscape that defines asexual and sexual *Plasmodium falciparum* parasites. Sci Rep 7:607. https://doi.org/10.1038/s41598-017-00687-7

30. von Grüning H, Coradin M, Mendoza MR, Reader J, Sidoli S, Garcia BA, Birkholtz L-M. 2022. A dynamic and combinatorial histone code drives malaria parasite asexual and sexual development. Mol Cell Proteomics 21:100199. https://doi.org/10.1016/j.mcpro.2022.100199

31. Shrestha S, Lucky AB, Brashear AM, Li X, Cui L, Miao J. 2022. Distinct histone post-translational modifications during *Plasmodium falciparum* gametocyte development. J Proteome Res 21:1857–1867. https://doi.org/10.1021/acs.jproteome.2c00108

32. Rashidi S, Tuteja R, Mansouri R, Ali-Hassanzadeh M, Shafiei R, Ghani E, Karimazar M, Nguewa P, Manzano-Román R. 2021. The main post-translational modifications and related regulatory pathways in the malaria parasite *Plasmodium falciparum*: an update. J Proteomics 245:104279. https://doi.org/10.1016/j.jprot.2021.104279

33. Fisk JC, Read LK. 2011. Protein arginine methylation in parasitic protozoa. Eukaryot Cell 10:1013–1022. https://doi.org/10.1128/EC.05103-11

34. Fan Q, Miao J, Cui L, Cui L. 2009. Characterization of PRMT1 from *Plasmodium falciparum*. Biochem J 421:107–118. https://doi.org/10.1042/BJ20090185

35. Krause CD, Yang Z-H, Kim Y-S, Lee J-H, Cook JR, Pestka S. 2007. Protein arginine methyltransferases: evolution and assessment of their pharmacological and therapeutic potential. Pharmacol Ther 113:50–87. https://doi.org/10.1016/j.pharmthera.2006.06.007

36. Lucky AB, Wang C, Liu M, Liang X, Min H, Fan Q, Siddiqui FA, Adapa SR, Li X, Jiang RHY, Chen X, Cui L, Miao J. 2023. A type II protein arginine methyltransferase regulates merozoite invasion in *Plasmodium falciparum*. Commun Biol 6:659. https://doi.org/10.1038/s42003-023-05038-z

37. Coetzee N, von Grüning H, Opperman D, van der Watt M, Reader J, Birkholtz L-M. 2020. Epigenetic inhibitors target multiple stages of *Plasmodium falciparum* parasites. Sci Rep 10:2355. https://doi.org/10.1038/s41598-020-59298-4

38. Wang M, Tang T, Li R, Huang Z, Ling D, Zheng L, Ding Y, Liu T, Xu W, Zhu F, Min H, Boonhok R, Mao F, Zhu J, Li X, Jiang L, Li J. 2022. Drug repurposing of quisinostat to discover novel *Plasmodium falciparum* HDAC1 inhibitors with enhanced triple-stage antimalarial activity and improved safety. J Med Chem 65:4156–4181. https://doi.org/10.1021/acs.jmedchem.1c01993

39. Vanheer LN, Zhang H, Lin G, Kafsack BFC. 2020. Activity of epigenetic inhibitors against *Plasmodium falciparum* asexual and sexual blood stages. Antimicrob Agents Chemother 64:e02523-19. https://doi.org/10.1128/AAC.02523-19

40. Eram MS, Shen Y, Szewczyk M, Wu H, Senisterra G, Li F, Butler KV, Kaniskan HÜ, Speed BA, Dela Seña C, Dong A, Zeng H, Schapira M, Brown PJ, Arrowsmith CH, Barsyte-Lovejoy D, Liu J, Vedadi M, Jin J. 2016. A potent, selective, and cell-active inhibitor of human type I protein arginine methyltransferases. ACS Chem Biol 11:772–781. https://doi.org/10.1021/acschembio.5b00839

41. Shen Y, Szewczyk MM, Eram MS, Smil D, Kaniskan HÜ, de Freitas RF, Senisterra G, Li F, Schapira M, Brown PJ, Arrowsmith CH, Barsyte-Lovejoy D, Liu J, Vedadi M, Jin J. 2016. Discovery of a potent, selective, and cell-active dual inhibitor of protein arginine methyltransferase 4 and protein arginine methyltransferase 6. J Med Chem 59:9124–9139. https://doi.org/10.1021/acs.jmedchem.6b01033

42. Ferreira de Freitas R, Eram MS, Smil D, Szewczyk MM, Kennedy S, Brown PJ, Santhakumar V, Barsyte-Lovejoy D, Arrowsmith CH, Vedadi M, Schapira M. 2016. Discovery of a potent and selective coactivator associated arginine methyltransferase 1 (CARM1) inhibitor by virtual screening. J Med Chem 59:6838–6847. https://doi.org/10.1021/acs.jmedchem.6b00668

43. Duncan KW, Rioux N, Boriack-Sjodin PA, Munchhof MJ, Reiter LA, Majer CR, Jin L, Johnston LD, Chan-Penebre E, Kuplast KG, Porter Scott M, Pollock RM, Waters NJ, Smith JJ, Moyer MP, Copeland RA, Chesworth R. 2016. Structure and property guided design in the identification of PRMT5 tool compound EPZ015666. ACS Med Chem Lett 7:162–166. https://doi.org/10.1021/acsmedchemlett.5b00380

44. Gerhart SV, Kellner WA, Thompson C, Pappalardi MB, Zhang X-P, Montes de Oca R, Penebre E, Duncan K, Boriack-Sjodin A, Le B, Majer C, McCabe MT, Carpenter C, Johnson N, Kruger RG, Barbash O. 2018. Activation of the p53-MDM4 regulatory axis defines the anti-tumour response to PRMT5 inhibition through its role in regulating cellular splicing. Sci Rep 8:9711. https://doi.org/10.1038/s41598-018-28002-y

45. Brehmer D, Beke L, Wu T, Millar HJ, Moy C, Sun W, Mannens G, Pande V, Boeckx A, van Heerde E, et al. 2021. Discovery and pharmacological characterization of JNJ-64619178, a novel small-molecule inhibitor of PRMT5 with potent antitumor activity. Mol Cancer Ther 20:2317–2328. https://doi.org/10.1158/1535-7163.MCT-21-0367

46. Tao H, Yan X, Zhu K, Zhang H. 2019. Discovery of novel PRMT5 inhibitors by virtual screening and biological evaluations. Chem Pharm Bull 67:382–388. https://doi.org/10.1248/cpb.c18-00980

47. Chan-Penebre E, Kuplast KG, Majer CR, Boriack-Sjodin PA, Wigle TJ, Johnston LD, Rioux N, Munchhof MJ, Jin L, Jacques SL, et al. 2015. A selective inhibitor of PRMT5 with *in vivo* and *in vitro* potency in MCL

models. Nat Chem Biol 11:432–437. https://doi.org/10.1038/nchembio.1810

48. Tarighat SS, Santhanam R, Frankhouser D, Radomska HS, Lai H, Anghelina M, Wang H, Huang X, Alinari L, Walker A, Caligiuri MA, Croce CM, Li L, Garzon R, Li C, Baiocchi RA, Marcucci G. 2016. The dual epigenetic role of PRMT5 in acute myeloid leukemia: gene activation and repression via histone arginine methylation. Leukemia 30:789–799. https://doi.org/10.1038/leu.2015.308

49. Bonday ZQ, Cortez GS, Grogan MJ, Antonysamy S, Weichert K, Bocchinfuso WP, Li F, Kennedy S, Li B, Mader MM, Arrowsmith CH, Brown PJ, Eram MS, Szewczyk MM, Barsyte-Lovejoy D, Vedadi M, Guccione E, Campbell RM. 2018. LLY-283, a potent and selective inhibitor of arginine methyltransferase 5, PRMT5, with antitumor activity. ACS Med Chem Lett 9:612–617. https://doi.org/10.1021/acsmedchemlett.8b00014

50. Orben F, Lankes K, Schneeweis C, Hassan Z, Jakubowsky H, Krauß L, Boniolo F, Schneider C, Schäfer A, Murr J, et al. 2022. Epigenetic drug screening defines a PRMT5 inhibitor-sensitive pancreatic cancer subtype. JCI Insight 7:10. https://doi.org/10.1172/jci.insight.151353

51. Miao J, Wang C, Lucky AB, Liang X, Min H, Adapa SR, Jiang R, Kim K, Cui L. 2021. A unique GCN5 histone acetyltransferase complex controls erythrocyte invasion and virulence in the malaria parasite *Plasmodium falciparum*. PLoS Pathog 17:e1009351. https://doi.org/10.1371/journal.ppat.1009351

52. Rocamora F, Gupta P, Istvan ES, Luth MR, Carpenter EF, Kümpornsin K, Sasaki E, Calla J, Mittal N, Carolino K, Owen E, Llinás M, Ottilie S, Goldberg DE, Lee MCS, Winzeler EA. 2021. PfMFR3: a multidrug-resistant modulator in *Plasmodium falciparum*. ACS Infect Dis 7:811–825. https://doi.org/10.1021/acsinfecdis.0c00676

53. Lucky AB, Wang C, Li X, Chim-Ong A, Adapa SR, Quinlivan EP, Jiang R, Cui L, Miao J. 2023. Characterization of the dual role of *Plasmodium falciparum* DNA methyltransferase in regulating transcription and translation. Nucleic Acids Res 51:3918–3933. https://doi.org/10.1093/nar/gkad248

54. Kim H, Ronai ZA. 2020. PRMT5 function and targeting in cancer. Cell Stress 4:199–215. https://doi.org/10.15698/cst2020.08.228

55. Miranda Furtado CL, Dos Santos Luciano MC, Silva Santos RD, Furtado GP, Moraes MO, Pessoa C. 2019. Epidrugs: targeting epigenetic marks in cancer treatment. Epigenetics 14:1164–1176. https://doi.org/10.1080/15592294.2019.1640546

56. Feustel K, Falchook GS. 2022. Protein arginine methyltransferase 5 (PRMT5) inhibitors in oncology clinical trials: a review. J Immunother Precis Oncol 5:58–67. https://doi.org/10.36401/JIPO-22-1

57. Sabnis RW. 2021. Novel PRMT5 inhibitors for treating cancer. ACS Med Chem Lett 12:1537–1538. https://doi.org/10.1021/acsmedchemlett.1c00512

58. Gao J, Yang J, Xue S, Ding H, Lin H, Luo C. 2023. A patent review of PRMT5 inhibitors to treat cancer (2018 - present). Expert Opin Ther Pat 33:265–292. https://doi.org/10.1080/13543776.2023.2201436

59. Huang Z, Li R, Tang T, Ling D, Wang M, Xu D, Sun M, Zheng L, Zhu F, Min H, et al. 2020. A novel multistage antiplasmodial inhibitor targeting *Plasmodium falciparum* histone deacetylase 1. Cell Discov 6:93. https://doi.org/10.1038/s41421-020-00215-4

60. Siddiqui FA, Boonhok R, Cabrera M, Mbenda HGN, Wang M, Min H, Liang X, Qin J, Zhu X, Miao J, Cao Y, Cui L. 2020. Role of *Plasmodium falciparum* Kelch 13 protein mutations in *P. falciparum* populations from northeastern Myanmar in mediating artemisinin resistance. MBio 11:e01134-19. https://doi.org/10.1128/mBio.01134-19

61. Waterhouse A, Bertoni M, Bienert S, Studer G, Tauriello G, Gumienny R, Heer FT, de Beer TAP, Rempfer C, Bordoli L, Lepore R, Schwede T. 2018. SWISS-MODEL: homology modelling of protein structures and complexes. Nucleic Acids Res 46:W296–W303. https://doi.org/10.1093/nar/gky427

62. Jumper J, Evans R, Pritzel A, Green T, Figurnov M, Ronneberger O, Tunyasuvunakool K, Bates R, Žídek A, Potapenko A, et al. 2021. Highly accurate protein structure prediction with AlphaFold. Nature New Biol 596:583–589. https://doi.org/10.1038/s41586-021-03819-2

63. Varadi M, Anyango S, Deshpande M, Nair S, Natassia C, Yordanova G, Yuan D, Stroe O, Wood G, Laydon A, et al. 2022. AlphaFold protein structure database: massively expanding the structural coverage of protein-sequence space with high-accuracy models. Nucleic Acids Res 50:D439–D444. https://doi.org/10.1093/nar/gkab1061

64. Hsiao K, Zegzouti H, Goueli SA. 2016. Methyltransferase-glo: a universal, bioluminescent and homogenous assay for monitoring all classes of methyltransferases. Epigenomics 8:321–339. https://doi.org/10.2217/epi.15.113